Inorg. Chem. **2007**, *46*, 5372–5380

Synthesis and Antimicrobial Activities of Isomers of *N*(4),*N*(11)-Dimethyl-3,5,7,7,10,12,14,14-octamethyl-1,4,8,11-tetraazacyclotetradecane and Their Nickel(II) Complexes

Tapashi G. Roy,*,† Saroj K. S. Hazari,† Benu K. Dey,† Hazarat A. Miah,† Falk Olbrich,‡ and Dieter Rehder*,‡

Departments of Chemistry, University of Chittagong, Chittagong-4331, Bangladesh, and University of Hamburg, D-20146 Hamburg, Germany

Received September 8, 2006

The reactions of two isomers of 3,5,7,7,10,12,14,14-octamethyl-1,4,8,11-tetraazacyclotetradecane (differing in the orientation of the methyl groups on the chiral carbon atoms), designated as L_B and L_C, with CH_3I in the ratio of 1:4 resulted in the substitution of the N(4) and N(11) protons by CH_3 groups, forming the dimethyl derivatives L_{BZ} and L_{CZ}, respectively. These ligands, on interaction with nickel(II) acetate tetrahydrate and subsequent addition of lithium perchlorate, produce square-planar yellow $[NiL_{BZ}][ClO_4]_2$ and orange $[NiL_{C'Z}][ClO_4]_2$. These nickel complexes undergo axial ligand addition reactions with NCS^-, Cl^-, Br^-, and I^- as X^- to form six-coordinate *trans*-diisothiocyanato, -dichloro, -dibromo, and -diiodo complexes of formula $[NiLX_2]$, where L = L_{BZ} or $L_{C'Z}$, and X = SCN, Cl, Br, or I. All these compounds have been characterized on the basis of analytical, spectroscopic, conductometric, and magnetochemical data. The structures of L_{BZ} and two variants of $[Ni"L_{BZ}"][ClO_4]_2$ (crystallizing in the space group $P2_1/n$ and Pn, respectively; "L_{BZ}" symbolizes partially methylated ligand) have been determined by single-crystal X-ray analyses. The antifungal and antibacterial activities of these compounds have been studied against some phytopathogenic fungi and bacteria.

1. Introduction

The natural macrocyclic metal complexes like the porphinogenes of hemoglobin and other heme proteins, chlorophyll, vitamin B_{12}, and the Ni-containing cofactor F_{430} in methanogenesis are structurally complex systems. Generally and simplistically, these systems may be considered as rigid planar cyclic structures carrying additional pendent functional groups which act as structural, axial components at the coordination sites.[1,2] The design and synthesis of simple macrocyclic systems carrying comparable functional groups mimicking the properties of their natural counterparts is a multifarious problem.

To synthesize the requisite type of macrocycles, the obvious approach is to first synthesize the simple macrocyclic ligand, and then to attach suitable pendent (functionalized) hydrocarbon moieties to the periphery of these macrocycles through appropriate reactions. For this purpose, syntheses and characterization of the simple isomeric macrocyclic ligands L_A−L_C have been carried out.[3,4] The suffixes A−C indicate differing orientations of the methyl groups on C3, C5, C10, and C12. In L_A, all of these methyl groups are oriented equatorially, in L_B, they are alternately equatorial and axial, and in L_C, one is axial while three are in equatorial positions (for L_B and L_C; cf. Scheme 1 in the Results and Discussion). In addition, a number of macrocycles carrying N-substituents have been prepared by alkylation reactions.[5]

To investigate variations of the ligating ability of the isomeric tetraaza N-donor macrocycles Me_8[14]ane

* To whom correspondence should be addressed. E-mail: tapashir@yahoo.com (T.G.R.).
† University of Chittagong.
‡ University of Hamburg.

(1) Pillsbury, D. G.; Bush, D. H. *J. Am. Chem. Soc.* **1976**, *98*, 7836 − 7839.
(2) Schammel, W. P.; Mertes, K. S. B.; Christoph, G. G.; Bush, D. H. *J. Am. Chem. Soc*. **1979**, *101*, 1622−1623.
(3) Roy, T. G.; Bembi, R. *J. Bangl. Chem. Soc*. **2002**, *15*, 23−29; *Chem. Abstr*. **2003**, *139*, 230266.
(4) Bembi, R. S.; Sondhi, M.; Singh, A. K.; Singh, R.; Roy, T. G.; Jhanji, A. K.; Lown, J. W.; Ball, R. G. *Bull. Chem. Soc. Jpn.* **1989**, *62*, 3701−3705.
(5) (a) Hay, R. W.; Bembi, R. *Inorg. Chim. Acta* **1982**, *65*, L227−L230. (b) Medeyski, C. M.; Micheal, J. P.; Hancock, R. D. *Inorg. Chem*. **1984**, *23*, 1487−1489. (c) Wainwright, K. P. *J. Chem. Soc., Dalton Trans*. **1983**, 1149−1152. (d) Clarke, P.; Lincoln, S. F.; Wainwright, K. P. *Inorg. Chem.* **1991**, *30*, 134−139.

10.1021/ic061700t CCC: $37.00
Published on Web 06/01/2007

Scheme 1

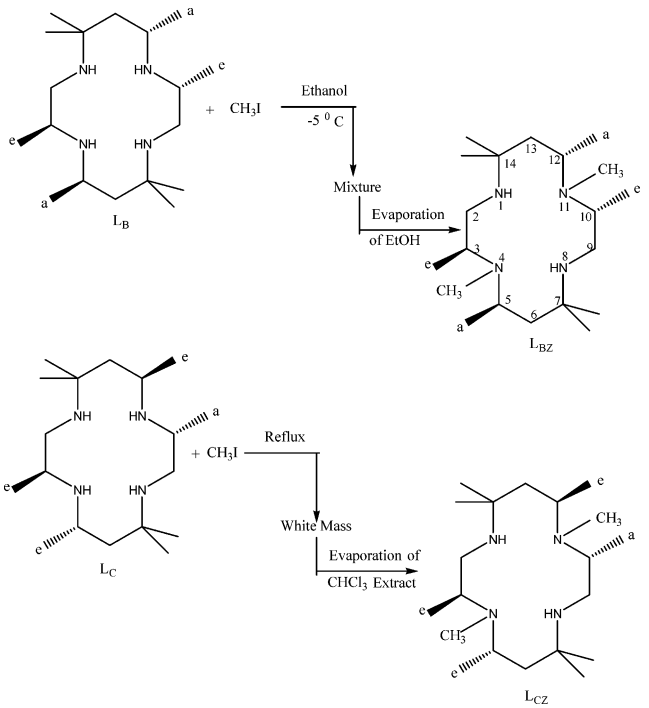

(L_A-L_C), attempts have been undertaken to synthesize variants of the ligands by substituting protons of the N−H groups by pendent functional groups which have coordinating abilities and/or influence the ligating ability of the original N-donor ligands. Thus, in the reactions of L_B with acrylonitrile, and of L_B and L_C with ethylene oxide, two NH-protons could be substituted by two $-CH_2CH_2CN$[6] and $-CH_2CH_2OH$[7] groups, respectively, to yield the bis(2-cyanoethyl) (L_{BX}) and the bis(2-hydroxyethyl) (L_{BY}, L_{CY}) derivatives. The structures of L_{BX}[6] and L_{BY}[7] have been confirmed by X-ray crystallography. In a similar way, the reactions of CH_3I with L_B and L_C at −5 °C and under reflux produced products having the empirical formula $C_{20}H_{44}N_4$ corresponding to $[(L_B - 2H)(CH_3)_2]$ and $[(L_C - 2H)(CH_3)_2]$. These newly formed dimethyl derivatives are denoted L_{BZ} and L_{CZ}.

Recently, studies on the square planar copper(II) and nickel(II) complexes of the N-pendent ligands L_{BX}, L_{BY}, and L_{AY} of composition $[ML][ClO_4]_2$ have been carried out.[7,8] It thus seemed likely that similar complexes of metal ions can be prepared with the dimethyl derivatives L_{BZ} and L_{CZ}. In this context, synthesis, characterization, and antimicrobial activities of L_{BZ} and L_{CZ}, their four-coordinate nickel(II) complexes of formula $[NiL][ClO_4]_2$, and their axial addition products of general formula $[NiLX_2]$ (X = SCN, Cl, Br, or I) are reported.

2. Experimental Section

2.1. Materials and Equipment. All chemicals were of analytical reagent grade and used without further purification.

Caution! Perchlorates can be explosive at high temperature and in the presence of organic materials.

Microanalyses (C, H, N) have been carried out on a CHNS analyzer at the Analytical Section of the Chemistry Department, University of Hamburg. For nickel, a standard complexometric titration with EDTA has been employed. Infrared spectra were taken as KBr pellets in the range 4000−400 cm^{-1} on a Perkin-Elmer 883 IR spectrometer. Electronic absorption spectra were recorded on a Schimadzu UV−visible spectrophotometer. The mass spectral measurements of the ligands were carried out with the help of a Varian MAT 311A (70 eV, EI) instrument. ^1H and ^{13}C NMR spectra were recorded on a 200 MHz Varian Gemini instrument. Conductance measurements of the metal complexes were done in water, acetonitrile, and chloroform solutions, using a HANNA instrument equipped with a HI 8820N conductivity cell. Magnetic measurements were carried out with a Gouy balance, calibrated against Hg-$[Co(NCS)_4]$; susceptibilities were corrected for diamagnetic increments.

2.2. Syntheses of Macrocycles. Synthesis of the parent ligand, 3,10-*C*-*meso*-Me_8[14]diene dihydroperchlorate,[9] reduction of this diene, and separation of the isomeric Me_8[14]anes were carried out to produce L_A-L_C according to literature methods.[3,4]

The bis(N-methyl) derivatives L_{BZ} and L_{CZ} of the isomeric L_B and L_C ligands were synthesized by modified literature methods adopted for analogous N-pendent ligands[10,11] as follows.

2.2.1. *trans*-3,5,7,7,10,12,14,14-Octamethyl-N^4,N^{11}-dimethyl-1,4,8,11-tetraazacyclotetradecane (L_{BZ}). A 0.312 g (1.0 mmol) amount of of L_B and 0.568 g (4.0 mmol) of methyl iodide were separately dissolved in 30 mL of absolute ethanol. At a temperature of −5 °C, the solutions were mixed. The colorless reaction mixture was stirred on a magnetic stirrer for about 3 h, maintaining the temperature constant. The solvent was removed on a rotary evaporator to yield white solid L_{BZ}, which was recrystallized from 5 mL of methanol−chloroform (1:1) and dried over silica gel under vacuum. Melting point: 170 °C. Yield: 0.153 g (45%). Anal. Calcd ($C_{20}N_4H_{44}$, M = 340.60 g mol^{-1}): C, 70.53; H, 13.02; N, 16.45. Found: C, 69.66; H, 12.92; N, 16.45.

2.2.2. *trans*-3,5,7,7,10,12,14,14-Octamethyl-N^4,N^{11}-dimethyl-1,4,8,11-tetraazacyclotetradecane (L_{CZ}). A 0.312 g (1.0 mmol) amount of L_C and 0.568 g (4.0 mmol) of methyl iodide were separately dissolved in 30 mL of dry ethanol. The methyl iodide solution was added dropwise to the L_C solution at room temperature with stirring, followed by refluxing for 3−4 h. A white precipitate formed, which was separated by filtration and washed with ethanol. The white crystalline solid was transferred to a 250 mL beaker, and 50 mL of aqueous NaOH was added to raise the pH above 12. From this mixture, the ligand L_{CZ} was extracted with chloroform. The chloroform extract was evaporated on a steam bath to yield white solid L_{CZ}. This was recrystallized from 5 mL of chloroform−methanol (1:1) and finally dried under vacuum over silica gel. Mp: 135 °C. Yield: 0.187 g (55%). Anal. Calcd ($C_{20}N_4H_{44}$, M = 340.60 g mol^{-1}): C, 70.53; H, 13.02; N, 16.45. Found: C, 70.49; H, 13.00; N, 16.36.

2.3. Syntheses of Nickel(II) Complexes. 2.3.1. Syntheses of the Complexes $[NiL][ClO_4]_2$ (L = L_{BZ} or $L_{C'Z}$). 2.3.1.1. $[NiL_{BZ}][ClO_4]_2$. A 0.340 g (1.0 mmol) amount of L_{BZ} and 0.256 g (1.05 mmol) of nickel(II) acetate tetrahydrate were dissolved separately in 50 mL of cold and dry methanol. The ligand solution was added

(6) Roy, T. G.; Hazari, S. K. S.; Dey, B. K.; Miah, H. A.; Tiekink, E. R. T. *Acta Crystallogr.* **2001**, *E57*, 524−525.
(7) Roy, T. G.; Hazari, S. K. S.; Dey, B. K.; Miah, H. A.; Bader, C.; Rehder, D. *Eur. J. Inorg. Chem.* **2004**, 4115−4123.
(8) Meah, H. A. Ph.D. Thesis, Dept. of Chemistry, Chittagong University, Chittagong, Bangladesh, 2003.
(9) Curtis, N. F.; Swann, D. A.; Waters, T. N.; Maxwell, I. E. *J. Am. Chem. Soc.* **1969**, *91*, 4588−4589.
(10) Barefield, E. K.; Wagner, F. *Inorg. Chem.* **1973**, *12*, 2435−2439.
(11) Barefield, E. K.; Mocella, M. T. *J. Am. Chem. Soc.* **1975**, *97*, 4238−4246.

Table 1. Structure and Refinement Data for L_{BZ} and [Ni"L_{BZ}"][ClO_4]$_2$

param	L_{BZ}	[Ni"L_{BZ}"][ClO_4]$_2$, variant **1**	[Ni"L_{BZ}"][ClO_4]$_2$, variant **2**
empirical formula	$C_{20}H_{44}N_4$	$C_{18.73}H_{41.46}Cl2N_4NiO_8$	$C_{18.67}H_{41.34}C_{l2}N_4NiO_8$
fw	340.59	580.39	579.55
cryst system	monoclinic	monoclinic	monoclinic
space group	$P2_1/c$	Pn	$P2_1/n$
unit cell dimens			
a, Å	8.6004(11)	10.3722(7)	10.3621(10)
b, Å	11.0851(14)	8.7631(6))	8.7516(8)
c, Å	11.4738(14)	14.1379(10)	14.1248(13)
β, deg	108.214(2)	100.0940(10)	100.130(2)
cell vol, Å^3	*1039.6(2)*	*1265.14(15)*	*1260.9(2)*
Z	2	2	2
calcd density, g/mL	1.088	1.524	1.526
abs coeff, mm^{-1}	0.065	1.028	1.032
cryst size, mm	0.60 × 0.43 × 0.17	0.53 × 0.36 × 0.34	0.34 × 0.31 × 0.17
θ range for data collcn, deg	2.49−26.98	2.26−27.50	2.26−27.50
index ranges	$-10 < h < 7$, $-13 < k < 14$, $-14 < 1 < 14$	$-13 < h < 13$, $-8 < k < 11$, $-18 < 1 < 15$	$-13 < h < 13$, $-11 < k < 9$, $-18 < 1 < 16$
reflcns collcd	6514	8150	8172
indpndt reflcns	2238 (R_{int} = 0.0292)	4623 (R_{int} = 0.0276)	2837 (R_{int} = 0.0351)
goodness-of-fit on F^2	1.000	1.002	1.001
final R indices [$I > 2\sigma(I_0)$]	R1 = 0.0454 $wR2$ = 0.1119	R1 = 0.0318 $wR2$ = 0.754	R1 = 0.0521 $wR2$ = 0.1690
R indices (all data)	R1 = 0.0643 wR2 = 0.1176	R1 = 0.0336 wR2 = 0.0763	R1 = 0.0627 wR2 = 0.1768
largest diff peak and hole, e Å^{-3}	0.276 and −0.175	0.363 and −0.248	0.478 and −0.852
CCDC no.	608062	610270	610154

dropwise to the boiling solution of the nickel(II) acetate with stirring. The reaction mixture was heated on a steam bath for 1 h and the volume reduced to 20 mL. An orange color developed. After addition of 0.5 g of lithium perchlorate trihydrate, the solution was again heated for 10 min and allowed to stand for about 2 h. The yellow product [NiL_{BZ}][ClO_4]$_2$ was filtered off, washed with methanol, followed by diethyl ether, and dried under vacuum. Yield: 0.477 g (80%). Anal. Calcd ($C_{20}N_4H_{44}NiCl_2O_8$, M = 596.19 g mol^{-1}): C, 40.16; H, 7.41; N, 9.37; Ni, 9.81. Found: C, 40.00; H, 7.13; N, 9.29; Ni, 9.72.

2.3.1.2. [Ni$L_{C'Z}$][ClO_4]$_2$. A 0.340 g (1.0 mmol) amount of L_{CZ} and 0.256 g (1.05 mmol) of nickel(II) acetate tetrahydrate were dissolved separately in 50 mL of cold and dry methanol. The ligand solution was added dropwise to the boiling nickel(II) acetate solution with stirring. A yellow color developed within 20 min, and by heating of the sample on a steam bath, the volume was reduced to 40 mL, followed by addition of 0.5 g of lithium perchlorate trihydrate. The reaction mixture was evaporated to dryness and the yellow product extracted with hot acetonitrile. The yellow extract, on evaporation on a steam bath, yielded orange-yellow [Ni$L_{C'Z}$][ClO_4]$_2$. This product was recrystallized from 7 mL of acetonitrile−methanol (1:1) and dried under vacuum over silica gel. Yield: 0.387 g (65%). Anal. Calcd ($C_{20}N_4H_{44}NiCl_2O_8$, M = 598.19 g mol^{-1}): C, 40.16; H, 7.41; N, 9.37; Ni, 9.81. Found: C, 39.98; H, 7.11; N, 8.99; Ni, 9.75.

2.3.2. Synthesis of Axial Addition Products. The axial addition products were prepared from the square planar complexes [NiL]-[ClO_4]$_2$ (L = L_{BZ} or $L_{C'Z}$) by following a method adopted from Bembi and co-workers.[12] A representative procedure is described for the preparation of [NiL_{BZ}(NCS)$_2$]:

2.3.2.1. [NiL_{BZ}(NCS)$_2$]. A 0.299 g (0.5 mmol) amount of [NiL_{BZ}]-[ClO_4]$_2$ and 0.097 g (1.0 mmol) of KCNS were separately suspended in 25 mL of hot methanol and mixed while hot. The yellow mixture was stirred for about 2 h and evaporated to dryness on a water bath. Then the mixture was extracted with hot chloroform and undissolved substance rejected. On evaporation, the pink chloroform extract gave a pink-violet product, [NiL_{BZ}(NCS)$_2$]. Finally the product was recrystallized from 5 mL of a chloroform−methanol (1:1) mixture and dried over silica gel in a vacuum desiccator. Yield: 0.168 g (65%). Anal. Calcd ($C_{22}N_6H_{44}NiS_2$, M = 515.44 g mol^{-1}): C, 51.27; H, 8.60; N, 16.30; Ni, 11.39. Found: C, 50.99; H, 8.54; N, 16.12; Ni, 11.05.

The following compounds were prepared accordingly:

[Ni$L_{C'Z}$(NCS)$_2$]: yield = 0.180 g (70%) of a violet product. Anal. Calcd ($C_{22}N_6H_{44}NiS_2$, M = 515.44 g mol^{-1}): C, 51.27; H, 8.60; N, 16.30; Ni, 11.39. Found: C, 51.00; H, 8.49; N, 16.10; Ni, 11.21.

[NiL_{BZ}Cl$_2$]: yield = 0.136 g (58%) of a blue solid. Anal. Calcd ($C_{20}N_4H_{44}NiCl_2$, M = 470.19 g mol^{-1}): C, 51.09; H, 9.43; N, 11.92; Ni, 12.48. Found: C, 50.96; H, 9.40; N, 11.73; Ni, 11.98.

[Ni$L_{C'Z}$Cl$_2$]: yield = 0.141 g (60%) of a violet-pink solid. Anal. Calcd ($C_{20}N_4H_{44}NiCl_2$, M = 470.19 g mol^{-1}): C, 51.09; H, 9.43; N, 11.92; Ni, 12.48. Found: C, 51.06; H, 9.45; N, 11.88; Ni, 12.25.

[NiL_{BZ}Br$_2$]: yield = 0.154 g (55%) of an orange-yellow product. Anal. Calcd ($C_{20}N_4H_{44}NiBr_2$, M = 559.09 g mol^{-1}): C, 42.97; H, 7.93; N, 10.02; Ni, 10.50. Found: C, 42.89; H, 7.03; N, 9.99; Ni, 10.40.

[Ni$L_{C'Z}$Br$_2$]: yield = 0.139 g (50%) of violet product. Anal. Calcd ($C_{20}N_4H_{44}NiBr_2$, M = 559.09 g mol^{-1}): C, 42.97; H, 7.93; N, 10.02; Ni, 10.50. Found: C, 42.86; H, 7.10; N, 9.96; Ni, 10.46.

[NiL_{BZ}I$_2$]: yield = 0.202 g (62%) of a violet solid. Anal. Calcd ($C_{20}N_4H_{44}NiI_2$, M = 653.10 g mol^{-1}): C, 36.78; H, 6.79; N, 8.58; Ni, 8.99. Found: C, 36.49; H, 6.00; N, 8.37; Ni, 8.87.

[Ni$L_{C'Z}$I$_2$]: yield = 0.192 g (59%) of a violet solid. Anal. Calcd ($C_{20}N_4H_{44}NiI_2$, M = 653.10 g mol^{-1}): C, 36.78; H, 6.79; N, 8.58; Ni, 8.99. Found: C, 36.49; H, 6.10; N, 8.44; Ni, 8.88.

2.4. X-ray Structure Analyses. Crystals of L_{BZ} suitable for the X-ray diffraction study were prepared by slow evaporation of a chloroform−methanol solution of the compound. [Ni"L_{BZ}"][ClO_4]$_2$ crystallized on slow evaporation of acetonitrile−methanol solutions of the complexes.

X-ray structure analyses were carried out at 153 K using Mo Kα radiation (λ = 0.710 73 Å, graphite monochromator) on an AXS SMART APEX diffractometer. H atoms were placed into calculated positions and refined with isotropic temperature factors

(12) Bembi, R.; Singh, R.; Roy, T. G.; Jhanji, A. K. *J. Coord. Chem.* **1985**, *14*, 119−126.

in the last cycles of refinement. The program package SHELXTL was used throughout for the solution and refinement of the structure. Absorption corrections were carried out with SADABS. In [Ni"L_{BZ}"][ClO_4]$_2$, the average number of methyl groups per ligand is 0.67−0.73 (instead of the required 2 for L_{BZ}); see text for details. Each of the perchlorate anions is disordered over two positions. Crystal and refinement data and CCDC numbers are collated in Table 1.

2.5. Antifungal Activity Test. The in vitro antifungal activities of the complexes against selected phytopathogenic fungi were assessed by the poisoned food technique. Potato dextros agar (PDA) was used as a growth medium. Dimethylformamide (DMF) was used as the solvent to prepare solutions of [Ni"L_{BZ}"][ClO_4]$_2$ complexes, and chloroform ($CHCl_3$), for the ligands and axial substitution products. The solutions were then mixed with the sterilized PDA so as to maintain concentrations of the compounds of 0.01%. A 20 mL volume of these solutions was each poured into a Petri dish. After the medium had solidified, a 5 mm micelial disc of each fungus was placed in the center of each assay plate, along with a control. Linear growth of the fungus was measured in mm after 5 days of incubation at 25 ± 2 °C.

2.6. Antibacterial Activity Test. The antibacterial activities of the test materials were measured by the disc diffusion method. Paper discs of 6 mm diameter and Petri plates of 70 mm in diameter were used throughout. Pour plates were prepared from sterilized molten nutrient agar (NA) at 45 °C. After solidification of the pour plates, suspensions of the test organisms were spread uniformly over the pour plate with a sterilized glass rod. After the paper discs were soaked with the test chemicals (1% in $CHCl_3$ solutions), they were placed in the center of the inoculated pour plate. A control plate was maintained in each case with $CHCl_3$ only. The plates were kept for 4 h at low temperature (4 °C) to allow the test chemicals to diffuse from the paper disc to the surrounding medium. The plates were then incubated at 35 ± 2 °C for growth of the test organisms and checked at 24-hours intervals. The antibacterial activity was expressed in terms of the diameter (in mm) of the zone of inhibition. Each experiment was repeated three times.

3. Results and Discussion

On the basis of MS,[3] ^{1}H NMR spectra,[4] and X-ray crystallography,[4] the structures of L_B and L_C, differing in the orientation of the methyl groups on the secondary carbons (equatorial e vs axial a), have been assigned as shown in Scheme 1. The reactions of CH_3I with L_B and L_C produced white products of the empirical formula $C_{20}H_{44}N_4$, corresponding to [(L_B − 2H)(CH_3)$_2$] and [(L_C − 2H)(CH_3)$_2$], designated as L_{BZ} and L_{CZ}, respectively. L_{BZ} and L_{CZ}, on interaction with nickel(II) acetate and subsequent treatment with lithium perchlorate, produce the square planar nickel(II) complexes [NiL_{BZ}][ClO_4]$_2$ and [$NiL_{C'Z}$][ClO_4]$_2$. These complexes undergo axial addition reactions with SCN^-, Cl^-, Br^-, and I^- to form the corresponding six-coordinate trans derivatives [$NiLX_2$] (L = L_{BZ} or $L_{C'Z;}$ X = SCN, Cl, Br, or I).

All of the compounds have been characterized by IR, UV−vis, and NMR spectroscopy, as well as by analytical, magnetochemical, and conductance measurements and, in the case of L_{BZ} and [NiL_{BZ}][ClO_4]$_2$, by single-crystal X-ray diffraction analysis.

Since ^{1}H NMR spectra could not be measured for the octahedral paramagnetic nickel(II) complexes, the stereochemistry of the octahedral complexes is based on the plausible assumption that axial addition reaction takes place without a change in conformation and configuration of the ligands in the square planar precursor complexes.

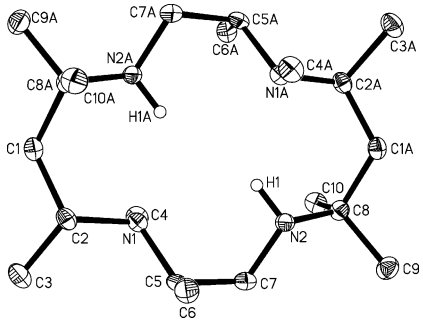

Figure 1. Molecular structure of the ligand L_{BZ}. Ellipsoids are drawn at the 30% probability level.

3.1. Ligands L_{BZ} and L_{CZ}. Reaction of CH_3I with L_B (Scheme 1) in the ratio 4:1 in ethanolic solution at −5 °C yielded L_{BZ} as a white microcrystalline powder. The same reaction with L_C under reflux produced a white product, the extraction of which with chloroform (at pH >12) and subsequent evaporation of the chloroform extract yielded L_{CZ}.

The analytical results demonstrated that in both cases only two N−H protons had been substituted by methyl groups. This conclusion is supported by ^{1}H NMR (Table 3), ^{13}C NMR (Table 4), and mass spectral analyses, which show that substitution of the NH-protons has taken place on N_4 and N_{11}, also confirmed by the X-ray structures of L_{BZ} (Figure 1) and [NiL_{BZ}][ClO_4]$_2$ (Figure 2). The positions of the substitution, *anti*-axial, are the same as in the case of the bis(2-hydroxyethyl) derivatives[7] but different from what has been observed for the bis(2-cyanoethyl) derivative.[6]

The IR spectra of the ligands show the ν_{N-H}, ν_{C-H}, ν_{C-C}, and ν_{CH_3} bands in the expected region (Table 2). Bands at 1365 and 1380 cm^{-1} indicate the presence of a *gem*-dimethyl. Usually, compounds containing the $-NCH_3$ group show a ν_{C-H} band[13] below 3000 cm^{-1}. C_{BZ} and L_{CZ} also display this ν_{C-H} at 2850 cm^{-1}.

The mass spectra (Table 3) of the isomeric ligands L_{BZ} and L_{CZ} display peaks at *m*/*z* 340 corresponding to their molecular ions. These isomeric ligands show essentially the same fragmentation pattern, but the intensities of the ion peaks are different. The prominent mode of fragmentation for L_{BZ} and L_{CZ} is α-cleavage, removal of a methyl radical, and removal of alkene cyanide by C−N bond rupture, followed by rearrangement of hydrogen.

The ^{1}H NMR spectrum of the ligand L_{BZ} shows two singlets at 0.992 and 1.15 ppm corresponding to six protons each, assigned to the *gem*-dimethyl groups. The spectrum also shows two doublets at 0.753 and 1.252 ppm, each corresponding to six protons. This requires that C3, C10 and C5, C12 are in a pairwise equivalent configuration. The upfield doublet at 0.753 can be assigned to equatorial methyls, and the downfield doublet at 1.252 ppm, to axial methyl groups. A broad singlet at 2.096 ppm (6H) corre-

(13) Nakamotto, K. *Infrared spectra of inorganic and coordination compounds*; John Wiley Publ.: New York, 1963.

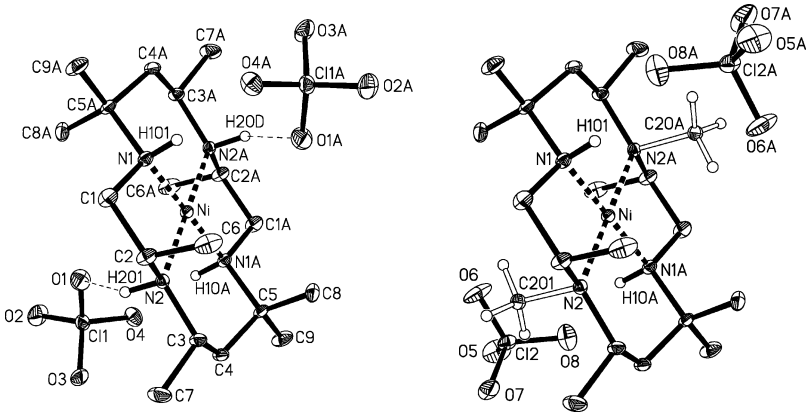

Figure 2. Drawing of the molecular structure of $[NiL_{BZ}/L_B][ClO_4]_2$ (30% probability level). Two limiting situations are shown: left, $[NiL_B][ClO_4]_2$; right, $[NiL_{BZ}][ClO_4]_2$.

Table 2. IR Spectral Data for the Ligands and Their Nickel(II) Complexes

	wavenumbers (cm^{-1}) and assgnt						
compd	ν_{N-H}	ν_{C-H}	ν_{CH_3}	ν_{C-C}	ν_{Ni-N}	ν_{ClO_4}	other bands
$C_{20}N_4H_{44}$ (L_{BZ})	3280	2950	1365	1150			
$C_{20}N_4H_{44}$ (L_{CZ})	3290	2950	1380	1150			
$[NiL_{BZ}][ClO_4]_2$	3187	2983	1383	1185	537	1102, 627	
$[NiL_{C'Z}][ClO_4]_2$	3191	2983	1344	1184	537	1184, 625	
$[NiL_{BZ}(NCS)_2]$	3226	2973	1344	1196	525		2010, ν_{CN}; 819, ν_{CS}; 454, δ_{NCS}
$[NiL_{C'Z}(NCS)_2]$	3220	2960	1370	1160	530		2080, ν_{CN}; 825, ν_{CS}; 467, δ_{NCS}
$[NiL_{BZ}Cl_2]$	3100	2980	1375	1140	580		
$[NiL_{C'Z}Cl_2]$	3180	2965	1365	1180	540		
$[NiL_{BZ}Br_2]$	3150	2985	1385	1150	570		
$[NiL_{C'Z}Br_2]$	3190	2960	1375	1185	545		
$[NiL_{BZ}I_2]$	3100	2980	1375	1140	580		
$[NiL_{C'Z}I_2]$	3180	2965	1365	1180	540		

Table 3. Mass Spectral Data for L_{BZ} and L_{CZ}

type	peaks for L_{BZ} at *m*/*z* (formula)	peaks for L_{CZ} at *m*/*z* (formula)
molecular ion	340 ($C_{20}H_{44}N_4$)	340 ($C_{20}H_{44}N_4$)
base	171 ($C_{10}H_{23}N_2$)	169 ($C_{10}H_{21}N_2$)
fragments	169 ($C_{10}H_{21}N_2$)	128 ($C_7H_{16}N_2$)
	126 ($C_7H_{14}N_2$)	127 ($C_7H_{15}N_2$)
	112 ($C_6H_{12}N_2$)	126 ($C_7H_{14}N_2$)
	98 ($C_5H_{10}N_2$)	112 ($C_6H_{12}N_2$)
	86 ($C_5H_{12}N$)	98 ($C_5H_{10}N_2$)
	58 (C_3H_8N)	58 (C_3H_8N)
	43 (C_2H_5N)	42 (C_2H_4N)
	42 (C_2H_4N)	

Table 4. ^1H NMR Spectra Data for the Ligands L_{BZ} and L_{CZ} and for $[NiL_{C'Z}][ClO_4]_2$

types of protons	L_{BZ} δ (ppm)[a]	$L_{C'Z}$ δ (ppm)[a]	$[NiL_{C'Z}][ClO_4]_2$ δ (ppm)[a]
gem-dimethyl	0.992 (s), 6H, e	0.994 (s), 6H, e	1.266 (s), 6H, e
	1.150 (s), 6H, a	1.050 (s), 6H, a	1.577 (s), 6H, a
methyl on chiral carbon atoms	0.753 (d), 6H, e	0.731 (d), 6H, e	1.068 (d), 6H, e
	1.251 (d), 6H, a	0.951 (d), 3H, e	1.504 (d), 6H, a
		1.156 (d), 3H, a	
CH_2, CH, and NH	1.978 (m)	1.980 (m)	
	2.112 (m)	2.311 (m)	
	2.533 (m)	2.980 (m)	
	2.547 (m)	3.041 (m)	
	2.563 (m)	3.310 (m)	
$-NCH_3$	2.096 (s, b)	2.026 (s)	
		2.520 (s)	

[a] s = singlet, d = doublet, m = multiplet, b = broad, a = axial, and e = equatorial.

sponds to the methyl groups at the nitrogens. The others α- and *β*-methylene and methine protons appear as poorly resolved multiplets at 1.978, 2.112, 2.202, 2.301, 2.533, 2.547, and 2.563 ppm (Table 4). The assignment follows that for the parent ligand L_B; the configuration is thus retained on conversion of L_B to L_{BZ}, not unexpectedly, because the small methyl groups are not supposed to give rise to changes in the stereochemistry.

The ^1H NMR spectrum of the ligand L_{CZ} shows two singlets at 0.994 and 1.050 ppm corresponding to six protons each, which can be assigned to the *gem*-dimethyl groups. Three doublets appear at 0.731, 0.951, and 1.156 ppm (Table 3) in the ratio 2:1:1 corresponding to 6, 3, and 3 protons. The doublet at 0.731 can be assigned to a pair of equivalent equatorial methyl groups, the doublet at 0.951 to an equatorial methyl, and the doublet at 1.156 to an axial methyl. Such an arrangement is possible if the C5 and C12 methyls are in a *C-meso* configuration and both occupy an equatorial position, while the C3 and C10 methyls, also *meso*, occupy an axial and equatorial position, respectively. The methylene, methine, and NH protons appear as multiplets at 1.980, 2.310, 2.980, 3.040, and 3.310 ppm. Two broad signals at 2.020 and 2.520 ppm (3H each) indicate the presence of *N*-methyl groups.

The ^{13}C NMR spectrum of L_{BZ} reveals 10 peaks. Out of these, the four peaks (Table 5) in the range of 15−26 ppm can be assigned to the peripheral eight (two times four) methyl carbons, reflecting—in accordance with the ^1H NMR—the pairwise equivalence of the carbons within the ligand L_{BZ}. The peak at 35 ppm is assigned to the C6 and C13 ring carbons, and the four peaks in the range of 40−55

Table 5. ^{13}C NMR Spectral Data for the Ligands L_{BZ} and L_{CZ}

types of carbons	L_{BZ} δ (ppm)	L_{CZ} δ (ppm)
peripheral	15.75, 18.75, 21.50, 25.50	11.02, 13.53, 15.44, 17.94, 18.44, 20.04, 25.30, 25.90
ring	35.00, 43.00, 45.00, 47.50, 54.80	29.98, 31.87, 41.07, 45.77, 6.19, 47.25, 47.72, 51.09, 52.42, 56.10
$-NCH_3$	69	69.29, 69.44

Table 6. Color and Molar Conductivity Data for the Nickel Complexes

		acetonitrile		chloroform		water	
complex	color of the solid	color	Λ^a	color	Λ^a	color	Λ^a
$[NiL_{BZ}][ClO_4]_2$	yellow	yellow	165			yellow	182
$[NiL_{C'Z}][ClO_4]_2$	orange-yellow	yellow	163			yellow	170
$[NiL_{BZ}(NCS)_2]$	pink-violet			pink-violet	0	yellow	134
$[NiL_{C'Z}(NCS)_2]$	violet			violet	0	yellow	158
$[NiL_{BZ}Cl_2]$	blue			blue	0	yellow	150
$[NiL_{C'Z}Cl_2]$	violet-pink			violet-pink	0	yellow	163
$[NiL_{BZ}Br_2]$	orange-yellow			orange- yellow	0	yellow	173
$[NiL_{C'Z}Br_2]$	violet			violet	0	yellow	207
$[NiL_{BZ}I_2]$	violet			violet	0	yellow	173
$[NiL_{C'Z}I_2]$	violet			violet	0	yellow	157

[a] Molar conductivity (Ω^{-1} cm^2 mol^{-1}) of ca. 10^{-3} M solution at 28 ± 2 °C.

ppm are assigned to the remaining ring carbons. The peak at 69 ppm belongs to the $N-CH_3$ carbons. Again, the NMR pattern shows that the stereochemistry of the parent L_B (nine ^{13}C NMR resonances[4]) remains unaffected.

In contrast to L_{BZ}, the ^{13}C NMR of L_{CZ} shows 20 peaks, which correspond to 20 nonequivalent carbon atoms, indicating C_1 symmetry of the molecule, also supported by its ^1H NMR spectrum. The eight signals in the range of 11−26 ppm can be assigned to the eight peripheral carbons, and the two signals at 29.98 and 31.87 ppm, to C6 and C13. The two $N-CH_3$ carbons show two signals at 69.29 and 69.44 ppm (Table 5). The eight signals in the range of 40−57 ppm represent the ring carbons. The parent ligand L_C gives rise to 18 signals for 18 nonequivalent carbons.

The structure assigned to L_{BZ} on the basis of its NMR spectra is in complete agreement with the one obtained from X-ray crystallographic studies. A perspective view of the molecule is presented in Figure 1, and bond length and bond angles are in Table 8. The ligand reveals a symmetric substitution pattern at the N atoms, with the methyl groups on the nitrogens adjacent to the chiral carbons and, hence, reverse to L_{BX}, where the nitrogens adjacent to the *gem*-dimethyls are methylated. The molecule is a *meso* isomer (C_i symmetry); C3 and C5 are in the *S*- and C10 and C12 are in the *R*-configurations. The methyl groups and hydrogens at the N are directed into the cavity, with an intraatomic distance $NH\cdots N(CH_3) = 2.240$ Å. The orientation of the CH_3groups on the N atoms of L_{BZ} differ from that of the bis(2-cyanoethyl) derivative L_{BX},[6] where the 2-cyanoethyl groups are disposed above and below the N_4 plane and thus directed away from the central cavity formed by the macrocyclic ring.

3.2. Nickel(II) Complexes $[NiL][ClO_4]_2$ (L = L_{BZ} or $L_{C'Z}$). The reaction of nickel(II) acetate tetrahydrate with L_{BZ} or L_{CZ} and subsequent addition of lithium perchlorate in methanolic solution yielded yellow and orange-yellow square planar $[NiL_{BZ}][ClO_4]_2$ and $[NiL_{C'Z}][ClO_4]_2$,respectively. As evidenced by ^1H NMR (vide infra) L_{CZ} undergoes a rearrangement of the methyls on the chiral carbons on complexation to form complexes containing $L_{C'Z}$. Infrared spectra of these complexes show a ν_{N-H} band around 3200 cm $^{-1}$ and the perchlorate bands around 1100 and 620 cm^{-1} (Table 2). In addition, there are the bands for ν_{N-H}, ν_{C-C}, ν_{Ni-N}, and ν_{CH_3} in the expected regions. The mass spectrum of $[NiL_{C'Z}][ClO_4]_2$ shows a low intensity molecular ion peak at m/z = 597.7

The molar conductivity values for $[NiL][ClO_4]_2$ of 163 ($L_{C'Z}$) and 165 (L_{BZ}) Ω^{-1} cm^2 mol^{-1} (Table 6) in acetonitrile correspond to 1:2 electrolytes; i.e., the two ClO_4^- ions are counterions not participating in coordination. Similar results have been found in aqueous solution.

The magneto−chemical measurements of the complexes $[NiL][ClO_4]_2$ are in agreement with square planar diamagnetic nickel(II). We assign structures **I** and **II** (Scheme 2) to the $[NiL_{BZ}]^{2+}$ and $[NiL_{C'Z}]^{2+}$ cations, respectively. The ^1H NMR spectrum of $[NiL_{C'Z}][ClO_4]_2$ (Table 3) shows two singlets at 1.266 and 1.577 ppm corresponding to 6H each, which originate from the two *gem*-dimethyl pairs. The spectrum further shows two doublets at 1.068 (6H) and 1.504 ppm (6H), which can be assigned to two pairwise equivalent equatorial and two axial methyl groups. Hence, $[NiL_{C'Z}][ClO_4]_2$ has two equatorially oriented and two axially oriented methyl groups, and structure **II** in Scheme 2 can be assigned to $[NiL_{C'Z}]^{2+}$, which thus attains the thermodynamically most stable trans-III type of structure with the six-membered (NiN_2C_3) rings in the chair conformation.[14] A corresponding assignment has been made for a nickel(II) complex of the parent ligand L_C.[15]

Scheme 2

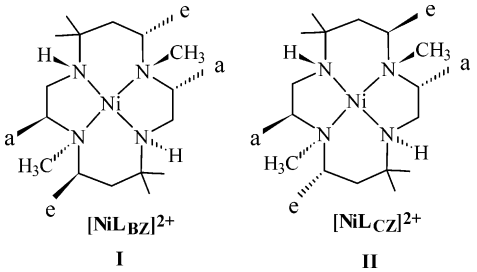

Table 7. UV−Vis Data for the Nickel Complexes[a]

complex	Nujol mull, λ_{max} (ϵ)	acetonitrile, λ_{max} (ϵ)	chloroform, λ_{max} (ϵ)	water, λ_{max} (ϵ)
$[NiL_{BZ}](ClO_4)_2$		477 (102), 243		
$[NiL_{C'Z}](ClO_4)_2$		468 (96), 240		
$[NiL_{BZ}(NCS)_2]$	620, 536, 248		910 (12), 792,259	450 (100), 240
$[NiL_{C'Z}(NCS)_2]$	758, 519, 442		914 (29), 745 (23), 250	452 (103), 235
$[NiL_{BZ}Cl_2]$[a]			772 (12), 492, 253	
$[NiL_{C'Z}Cl_2]$[a]			909, 763, 285	
$[NiL_{BZ}Br_2]$[a]			772 (5), 763, 253	
$[NiL_{C'Z}Br_2]$[a]			991, 946, 890 (14), 256	
$[NiL_{BZ}I_2]$[a]			989 (9), 763, 269	449 (99), 245
$[NiL_{C'Z}I_2]$[a]			989 (9)	456 (93), 255

[a] λ_{max} (nm) = wavelength of absorbance maxima in nm; ϵ = molar extinction coefficient in $dm^3\ mol^{-1}\ cm^{-1}$.

Table 8. Selected Bond Lengths (Å) and Angles (deg) for L_{BZ} and $[NiL_{BZ}][ClO_4]_2$

L_{BZ}		$[NiL_B/L_{BZ}][ClO_4]_2$ (variant **2**)	
		Ni−N1	1.951(3)
		Ni−N2	1.970(3)
N2−C7	1.451(2)	N1−C1	1.482(5)
N2−C8	1.476(2)	N1−C5a	1.523(4)
N1−C5	1.478(2)	N2−C2	1.503(5)
N1−C2	1.482(2)	N2−C3	1.500(4)
N1−C4	1.468(2)	N2−C201	1.521(12)
C5−C7	1.523(2)	C1−C2	1.503(5)
C1−C2	1.525(2)	C3−C4	1.509(5)
C1−C8a	1.533(2)	C4−C5	1.521(5)
		N1−Ni−N2	86.69(12)
		N1−Ni−N2a	93.31(12)
		Ni−N2−C2	106.5(2)
		Ni−N2−C201	102.3(4)
		Ni−N2−C3	123.7(2)
C2−N1−C5	113.85(10)	C3−N2−C2	111.4(3)
C2−N1−C4	111.80(10)	C3−N2−C201	107.2(5)
C5−N1−C4	111.11(10)	C2−N2−C201	103.7(5)
N1−C5−C7	111.02(10)	N2−C2−C1	105.4(3)
C5−C7−N2	111.63(11)	C2−C1−N1	107.8(3)
C7−N2−C8	116.57(10)	C1−N1−C5a	111.8(3)

The electronic spectra of these nickel(II) complexes display d−d bands at 468 and 477 nm (Table 7), which can be assigned to the $^1A_1g \rightarrow {}^1B_1g$ transition for square planar nickel(II) complexes. The results for our complexes fit well with those for complexes with other saturated macrocycles.[15] The relatively high ϵ_{max} values of 96 and 102 $dm^3\ mol^{-1}\ cm^{-1}$ in the visible region indicate that the complexes practically exclusively exist in the square planar geometry. Octahedral nickel(II) complexes give low extinction coefficients in the range of 20−30 $dm^3\ mol^{-1}\ cm^{-1}$. In the UV region, the absorption bands at 240 and 243 nm are assigned to charge-transfer transitions.

3.3. X-ray Structure Analysis of $[NiL_{BZ}/L_B][ClO_4]_2$. The crystals isolated from solutions of $[NiL_{BZ}][ClO_4]_2$ contained only partially methylated ligand. The methylation degree in two representative crystals described here, variant **1** (acentric space group) and variant **2** (centrosymmetric space group), was 36.5%, corresponding to 0.73 methyl groups/ligand in **1**, and 33.5%, corresponding to 0.67 methyl groups/ligand in **2**. No absolute statement can be made with respect to the different possibilities for the distribution of methyl groups, i.e., (i) a mixture of completely methylated (L_{BZ}), nonmethylated (L_B) and monomethylated ligand ($L_{BZ/2}$), and (ii) statistical methylation. The best convergence in the refinement was, however, obtained in the space groups *Pn* (for **1**) and $P2_1/n$ (for **2**), providing the following populations: variant **1**, 27% of unmethylated $[NiL_B][ClO_4]_2$ plus 73% of $[NiL_{BZ/2}][ClO_4]_2$, where $L_{BZ/2}$ refers to a ligand where only one of the nitrogens is methylated; variant **2**, 66.5% of unmethylated $[NiL_B][ClO_4]_2$ plus 33.5% of dimethylated $[NiL_{BZ}][ClO_4]_2$. The two possible limiting situations for variant **2**, $[NiL_B][ClO_4]_2$ and $[NiL_{BZ}][ClO_4]_2$, are depicted in Figure 2. Selected bond distances and angles are collated in Table 8.

The complex $[NiL_{BZ}][ClO_4]_2$ attains inversion symmetry; i.e., the atoms of the ligand in the cation $[NiL_{BZ}]^{2+}$ (Figure 2, right) are related by an inversion center located on Ni. Both perchlorate anions are disordered over two equivalent positions. The NH groups of the ligand L_B in $[NiL_B][ClO_4]_2$ are in hydrogen-bonding contact with the perchlorate oxo ions O1 and O1a (Figure 2, left). The geometry about the Ni^{2+} ions is square planar, defined by an N_4 donor set, with the methyl groups C6, C6a, C8, and C8a in axial positions, the methyl groups C7, C7a, C9, and C9a in equatorial positions, and the H/CH_3 at N2 and N2a mutually "down" and "up" with respect to the NiN_4 plane. As far as $[NiL_{BZ}][ClO_4]_2$ is concerned, the trans-III type of structure thus is realized.[15] This structure has been shown to be the most stable one for $[Co(RSSR\text{-}cyclam)Cl_2]^+$ and other comparable complexes.[7,16,17] The bond distances and angles for the complexes are in the normal range. The unique six-membered NiN_2C_3 rings adopt the chair configuration with the N−H and N−CH_3 moieties and the chiral methyls equatorially oriented. The five-membered NiN_2C_2 rings adopt the gauche conformation with the methyl groups in axial positions. The structure thus resembles those of analogous nickel(II) complexes.[15]

3.4. Axial Substitution Reaction Products. 3.4.1. Diisothiocyanatonickel(II) Complexes. NCS^- is a stronger ligand than Cl^-, Br^-, I^-, NO_2^-, and NO_3^-, and it was therefore expected that this ligand adds very easily to the axial sites of the square planar nickel(II) complexes. Extraction by chloroform of products produced by the reaction of $[NiL_{BZ}][ClO_4]_2$ and $[NiL_{C'Z}][ClO_4]_2$ with KNCS in the ratio

(14) Hay, R. W.; Bembi, R.; House, D. A. *J. Chem. Soc., Dalton Trans*. **1984**, 1921−1925.
(15) Roy, T. G.; Bembi, R.; Hazari, S. K. S.; Dey, B. K.; Acharjee, T. K.; Horn, E.; Tiekink, E. R. T. *J. Coord. Chem*. **2002**, *55*, 853−862.
(16) Bembi, R.; Drew, M. G. B.; Singh, R.; Roy, T. G. *Inorg. Chem*. **1991**, *30*, 1403−1406.
(17) Hambley, T. W. *J. Chem. Soc., Dalton Trans*. **1986**, 565−569.

1:2 and evaporation of the $CHCl_3$ extract yielded pink-violet and violet products, respectively.

Infrared spectra of the complexes $[NiL(NCS)_2]$ (L = L_{BZ} and $L_{C'Z}$) show all of the characteristics ν_{N-H}, ν_{C-C}, ν_{C-H}, ν_{Ni-N}, and ν_{CH_3} bands in the expected regions (Table 2). The presence of the ν_{CN} bands at 2010 and 2080, ν_{C-S} at 819 and 825, and δ_{NCS} at 454 and 467 cm^{-1} and the absence of the ν_{ClO4} bands at around 1100 and 620 cm^{-1} reveals that perchlorate is fully replaced by thiocyanate. The position of the ν_{CN} clearly indicates that the ligands are bonded through N, i.e., in the isothiocyanato fashion.[13]

The conductivity values (Table 5) of 0 Ω^{-1} cm^2 mol^{-1} for these complexes in $CHCl_3$ strongly support the nonelectrolytic nature of these complexes. The violet color of the complexes remains unchanged when dissolved in chloroform, indicating that they retain their geometry and conformation in this solvent. The conductivity values of 134 and 158 Ω^{-1} cm^2 mol^{-1} of the yellow aqueous solutions correspond to 1:2 electrolytes, providing evidence that water forces the anions out of the coordination sphere to form square planar complexes. The 1:2 electrolytes can be assigned either to square planar or to octahedral diaqua complexes; the square planar geometry is more likely, however, in the light of the square-planar 1:2 complexes $[NiL][ClO_4]_2$ forming yellow solutions in acetonitrile and water. Similar observation were noted in analogous systems.[12] Formation of square-planar complexes can be expressed by

$$[NiL(NCS)_2] \xrightarrow{H_2O} [NiL](NCS)_2 \quad L = L_{BZ} \text{ or } L_{C'Z} \quad (1)$$

The magnetic susceptibility values of the pure pink-violet and violet six-coordinate octahedral complexes could not be obtained since, on contact with moisture, they partly convert to the yellow square planar complexes. The μ_{eff} found, 0.65 (L_{BZ}) and 1.00 μ_B ($L_{C'Z}$), correspond to mixtures of or equilibria between the square-planar and octahedral forms. The electronic spectra of the complexes (Table 6) display d−d bands at about 450 nm with high extinction coefficients in aqueous solutions, which correspond to the square-planar complexes. In chloroform, d−d bands at 914−745 nm and low extinction coefficents[12] strongly support the octahedral geometry of the complexes in $CHCl_3$.

Since ^1H NMR spectra of the paramagnetic octahedral nickel(II) complexes are insufficiently informative with respect to structure elucidation, the structures of the complexes $[NiL(NCS)_2]$ have been assigned on the basis that once the square planar complexes have formed, addition of ligands at the axial sites does not change the configuration and conformation of the macrocyclic ligand framework of the original square-planar complexes. Thus, the probable structures of $[NiL_{BZ}(NCS)_2]$ and $[NiL_{C'Z}(NCS)_2]$ can be represented by **III** and **IV** in Scheme 3.

3.4.2. Dihalonickel(II) Complexes $[NiX_2]$/$[NiL]X_2$ (L = L_{BZ} or $L_{C'Z}$, X = Cl, Br or I). Reaction of $[NiL][ClO_4]_2$ with KCl in the ratio 1:2 yielded yellowish products. Extraction with chloroform and evaporation of the solvent gave blue (L_{BZ}) or violet-pink ($L_{C'Z}$) products. Exposed to air, these solids became yellowish, indicating a change of

Scheme 3

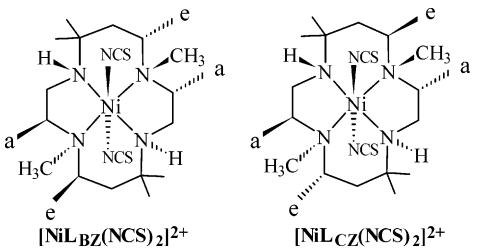

geometry. A comparable reaction takes place with KBr in methanol. Extraction of the yellowish masses with chloroform resulted in orange-yellow L_{BZ} and violet ($L_{C'Z}$) extracts which, on vacuum evaporation of the solvent, yielded equally colored products. On exposure to air, the yellowish products are immediately formed back. These dibromo complexes are more sensitive to air/moisture than the other axial addition products of this study, and they are less stable than the axial addition products of the nickel complexes of their parent ligands L_B and L_C.[19] This phenomenon may be explained by the fact that the ligands L_{BZ} and $L_{C'Z}$ are sterically more demanding due to the two additional methyl substituents on N. The reactions with KI provided violet solids. Again, the products changed to yellow on standing in air.

The infrared spectra (Table 2) of these complexes reveal bands due to ν_{N-H}, ν_{C-C}, ν_{C-H}, ν_{Ni-N}, and ν_{CH_3} in the expected regions. The absence of any bands at around 1100 and 620 cm^{-1} indicates that both the ClO_4^- ions are completely replaced by the halide ions. The molar conductivity values (Table 5) of 0 Ω^{-1} cm^2 mol^{-1} in chloroform is indicative of the nonelectrolytic nature of the complexes and thus supports the octahedral geometry of the products in nonaqueous solution. In contrast, the conductivity values of the yellow aqueous solutions corresponding to 1:2 electrolytes indicates the 100% conversion of the octahedral into square-planar species. Consequently, all of the halide complexes, when converted to their yellow form on exposure to air, are diamagnetic. The electronic spectra in chloroform display d−d bands which, along with the low ϵ values (Table 7), correspond to six-coordinate nickel(II) complexes. Accordingly, the violet forms (orange yellow in the case of $[NiL_{BZ}Br_2]$) can be formulated in analogy to the isothiocyanato complexes, viz. structures **III** and **IV** in Scheme 3.

3.5. Antifungal Activity Study. Studies on the antifungal activities of macrocycles and their complexes are restricted to a few recent reports.[7,18,20] We have therefore studied the antifungal activities of L_{BZ} and L_{CZ} and their nickel(II) complexes against the five selectively phytopathogenic fungi *Macrophomina phaseolina*, *Alternaria alternata*, *Fusarium equiseti*, *Colletotrichum corcolei*, and *Botryodiplodia theobromae*. The data are collated in Table 9. It is evident that the macrocycles and their complexes show some antifungal

(18) Roy, T. G.; Hazari, S. K. S.; Dey, B. K.; Chakraborty, S.; Tiekink, E. R. T. *Met. Based Drugs* **1999**, *6*, 345−354.
(19) Acharjee, T. K. M. Sc. Thesis, Dept. of Chemistry, Chittagong University, Chittagong, Bangladesh, 2000.
(20) Hazari, S. K. S.; Roy, T. G.; Dey, B. K.; Das, S. C.; Tiekink, E. R. T. *Met. Based Drugs* **1997**, *4*, 255−263.

Table 9. In Vitro Antifungal Activities of Ligands and Their Nickel Complexes

ligands and metal complexes	% inhibition of mycelial growth				
	M. phaseolina	*A. alternata*	*F. equiseti*	*C. corcolei*	*B. theobromae*
L_{BZ}	59.00	43.00	45.68	47.69	49.58
$[NiL_{BZ}][ClO_4]_2$	15.00	20.78	26.27	31.11	20.26
$[NiL_{BZ}(NCS)_2]$	7.78	9.00	14.00	12.36	21.63
$[NiL_{BZ}Cl_2]$	8.00	7.67	5.53	7.78	13.62
$[NiL_{BZ}Br_2]$	11.80	25.36	23.66	17.68	9.00
$[NiL_{BZ}I_2]$	2.00	0.00	2.50	2.80	23.36
$L_{C'Z}$	62.65	36.80	38.80	49.62	43.03
$[NiL_{C'Z}(NCS)_2]$	39.00	33.36	29.00	28.28	36.35
$[NiL_{C'Z}Cl_2]$	2.80	3.68	11.31	24.24	26.32
$[NiL_{C'Z}Br_2]$	11.60	0.00	3.06	22.55	27.00
$[NiL_{C'Z}I_2]$	9.20	2.68	13.77	26.31	31.68

Table 10. Antibacterial Activities

ligands and metal complexes	diameter of zone of inhibition in mm after 24 h			
	S. typhi	*Sh. dysenteriae*	*E. coli*	*B. cerelus*
L_{BZ}	00	00	00	00
$[NiL_{BZ}][ClO_4]_2$	06	04	03	07
$[NiL_{BZ}(NCS)_2]$	32	22	45	38
$[NiL_{BZ}Cl_2]$	05	04	06	nd
$[NiL_{BZ}Br_2]$	03	06	04	nd
$[NiL_{BZ}I_2]$	08	08	08	08
$L_{C'Z}$	00	00	00	00
$[NiL_{C'Z}][ClO_4]_2$	00	00	00	11
$[NiL_{C'Z}(NCS)_2]$	37	49	32	26
$[NiL_{C'Z}Cl_2]$	20	21	22	23
$[NiL_{C'Z}Br_2]$	12	02	23	21
$[NiL_{C'Z}I_2]$	31	22	12	00

activity. The activity of the ligands was found to decrease upon coordination to nickel(II) in all cases. Comparison of the activity of the systems studied here with that of sulfur-containing Schiff bases and their complexes[21,22] shows that the activity of the present ligands and complexes is lower. It has been noted that N-substituted ligands give rise to higher rates of inhibition on mycelial growth than their unsubstituted parent ligands,[20] and in the series of N-substituted ligands,[7,8] the inhibition rate is highest in case of the *N*-methyl-substituted ligands L_{BZ} and $L_{CZ.}$ The most prominent effect is observed for the inhibition on the growth of *M. phaseolina* by the ligands themselves. Further, the extent of inhibition by the complexes depends on the particular type of macrocyclic ligand (L_{BZ} vs $L_{C'Z}$) and the axial ligand/counterion (perchlorate, isothiocyanate, chloride, bromide, and iodide). The dependence on the axial ligand/counterion suggests that the six-coordinate species are present in equilibrium, even in these aqueous test media, also in the case of the halide complexes. Generally, the nickel(II) complexes exhibit higher activities than the corresponding cobalt(III) complexes of L_B and L_C.[23]

From the above discussion, it can be concluded that the nature of ligands, metals, and type of axial ligands/counterions plays a significant role in the inhibition of mycelial growth. However, to understand the functions responsible for antifungal activities of macrocycles and their complexes, more studies are necessary with a series of analogous ligands and their complexes.

3.6. Antibacterial Activity Study. Except for a single recent report,[7] antibacterial activities of macrocycles and their complexes have so far not been studied. Here, investigations on the antibacterial activity of the ligands and their nickel complexes have been carried out against selected bacteria, which can cause fatal diseases, viz. *Salmonella typhi, Shigella dysenteriae*, *Escherichia coli*, and *Bacillus cerelus*. The results (Table 10) show that while the ligands themselves are ineffective, several of their complexes exhibit antibacterial activity to some extent. This is in accord with observations on similar systems.[7] No systematic statements can be derived, however, on the inhibiting power of the complexes on a particular bacterial growth. For a clean understanding of the functions responsible for antibacterial activities of the macrocycles and their complexes, more studies are needed.

Acknowledgment. We thank the University Grants Commission of Bangladesh for a fellowship to H.A.M. and the Ministry of Science and Technology, Government of People's Republic of Bangladesh, for a grant to T.G.R. and for providing a fellowship to H.A.M. Grant of a stipend to T.G.R. by the German Academic Exchange Service (DAAD) is greatly acknowledged. We thank Prof. Dr. N. Anwar and Mr. M. S. Rahman, Department of Microbiology, University of Chittagong, for their support of the antifungal and antibacterial studies.

IC061700T

(21) Ali, M. A.; Mirza, A. H.; Monsur, A.; Hossain, S.; Nazimuddin, M. *Polyhedron* **2001**, *20*, 1045−1052.

(22) Hossain, M. E.; Alam, M. N.; Begum, J.; Ali, M. A.; Nazimuddin, M.; Smith, E. E.; Haynes, R. C. *Inorg. Chim. Acta* **1996**, *249*, 207−213.

(23) Roy, T. G.; Hazari, S. K. S.; Dey, B. K.; Sutradhar, R.; Dey, L.; Anowar, N.; Tiekink, E. R. T. J. *Coord. Chem. Rev.* **2006**, *59*, 351−362.